Colloids and Surfaces A: Physicochemical and Engineering Aspects 740 (2026) 140209

Contents lists available at ScienceDirect

Colloids and Surfaces A: Physicochemical and Engineering Aspects

journal homepage: www.elsevier.com/locate/colsurfa

Components interactions and stability factors in terpenes oil-in-water emulsions stabilized with hydrolyzed soybean lecithin

Andrea Casas González [a,b], Soraya Rodríguez-Rojo [a,b,*]

[a] BioEcoUVa, Research Institute on Bioeconomy, PressTech Group, University of Valladolid, Paseo Prado de la Magdalena 3-5, Valladolid 47011, Spain
[b] Dpt. of Chemical Engineering and Environmental Technology, Escuela de Ingenierías Industriales (sede Mergelina), Universidad de Valladolid, Pº Prado de la Magdalena 3-5, Valladolid 47011, Spain

HIGHLIGHTS

- Stable terpene oil-in-water emulsions achieved using water titration.
- Acidic pH alters stability through charge modification of lecithin and guar gum.
- Neutral pH maximizes viscoelastic reinforcement of the oil-water interfacial layer.
- Droplet stability controlled by polarity-driven interfacial and rheological behavior.
- Guar gum hydrogen-bond networks improve droplet separation and stability.

GRAPHICAL ABSTRACT

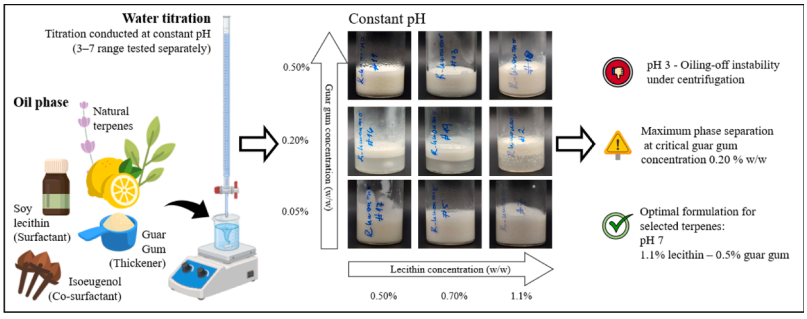

ARTICLE INFO

Keywords:
Terpenes
Low-energy emulsification methods
Hydrolyzed soy lecithin
Guar gum
Iso-eugenol
Phytosanitary products

ABSTRACT

R-(+)-limonene, eucalyptol, and linalool are natural compounds with promising antifungal activity but limited practical applicability due to high volatility, low water solubility, and photodegradability. This study investigates the formulation of stable oil-in-water emulsions using a low-energy phase inversion method and exclusively naturally derived components. The influence of the surfactant concentration (0.5–1.1 wt% hydrolyzed soybean lecithin), the addition of a co-surfactant (2.6 wt% isoeugenol), thickener concentration (0.05–0.50 wt% guar gum), continuous-phase pH (3, 5, & 7), and active compound physicochemical properties was systematically evaluated. Emulsions containing 11 wt% terpene were prepared by water titration. Stable formulations were obtained at neutral pH using 1.1 wt% lecithin, 2.6 wt% isoeugenol and 0.5 wt% guar gum. Acidification reduced stability, associated with pH-dependent variations in surface charge and intermolecular interactions affecting both interfacial organization and bulk rheology. Differences in droplet size distribution and viscosity among terpenes highlight the role of active compound polar character in governing emulsion microstructure. Overall, this work demonstrates that stable, fully natural terpene-based emulsions can be rationally designed using low-energy methods, providing a formulation framework relevant to sustainable phytosanitary applications.

* Corresponding author at: BioEcoUVa, Research Institute on Bioeconomy, PressTech Group, University of Valladolid, Paseo Prado de la Magdalena 3-5, Valladolid 47011, Spain.
E-mail address: soraya.rodriguez@uva.es (S. Rodríguez-Rojo).

https://doi.org/10.1016/j.colsurfa.2026.140209
Received 4 December 2025; Received in revised form 18 February 2026; Accepted 5 March 2026
Available online 7 March 2026

1. Introduction

International and European regulatory frameworks increasingly promote the reduction of synthetic pesticide use and encourage the adoption of safer and more sustainable phytosanitary strategies. In this context, biopesticides and biofungicides derived from natural sources are considered preferred alternatives due to their lower impact on human health and the environment [1-3]. Terpenes—biodegradable plant secondary metabolites—have attracted significant interest because of their antimicrobial and phytotoxic properties and their approval as active substances in several phytosanitary applications [4,5].

Among the terpenes currently authorized for phytosanitary applications, R-(+)-limonene, eucalyptol, and linalool are particularly relevant due to their widespread use, well-documented biological activity, and distinct physicochemical characteristics [6]. Due to their molecular structure (Fig. 1), these terpenes interact with biological membranes, conferring antimicrobial and phytotoxic activity [4,5]. However, the same structural features also govern their physicochemical behavior, which strongly influences their performance in formulated systems. These physicochemical limitations significantly hinder the direct application of terpenes in aqueous systems and highlight the need for formulation strategies capable of improving their dispersion, stability, and resistance to volatilization and degradation, among which colloidal delivery systems represent a particularly promising approach [7–9].

Emulsion-based formulations represent a widely adopted strategy to improve the dispersion and stability of hydrophobic active compounds in aqueous systems [9,14]. While high-energy emulsification methods can generate fine droplets through intense mechanical forces, low-energy approaches (such as phase inversion methods) offer an attractive alternative for thermally or mechanically sensitive compounds, as they rely on spontaneous droplet formation under controlled compositional conditions [14]. However, despite their advantages in terms of energy efficiency and process simplicity, low-energy emulsification methods are highly sensitive to formulation parameters, and achieving stable emulsions requires a detailed understanding of the interactions between surfactants, co-adjuvants, and the active compound [7,14,15].

Soy lecithin has been widely investigated as a natural emulsifier in oil-in-water systems due to its phospholipid composition, regulatory acceptance, and ability to self-assemble at the oil–water interface [6, 16–18]. However, despite these advantages, its application in low-energy emulsification methods remains challenging. Lecithin tends to form relatively rigid interfacial structures, resulting in a narrow formulation window. Therefore, in practice, it is not usually used alone and often requires synthetic non-ionic surfactants such as polysorbates or physicochemical adjustments, such as enzymatic modifications or pH adjustments, to achieve stable emulsions [19–22]. Previous studies have shown that enzymatic hydrolysis of soy lecithin or the incorporation of small polar co-components, such as some short-chain alcohols like glycerol, can enhance interfacial flexibility and emulsion stability. In this context, collaborative work from our research group demonstrated that both pure soybean lecithin and lecithin–glycerol mixtures enabled the formation of stable nanoemulsions of essential oils and pure compounds, yielding highly negative zeta potential values when processed by high-energy emulsification methods [23].

Isoeugenol is a phenylpropanoid containing a phenolic hydroxyl group (Fig. 1), which confers both biological activity and a degree of polarity. Its antimicrobial activity has been reported in pharmaceutical and biomedical contexts, where it is primarily associated with interactions with and disruption of biological membranes [4,24]. This membrane-disrupting behavior is thought to be related to the capacity to interact with lipid environments. With a moderate polar surface area (Table 1), isoeugenol has the potential to insert into and associate with phospholipid assemblies. Beyond its biological properties, the presence of a hydroxyl group in isoeugenol enables its interactions with both the aqueous phase and the interfacial region. As previously mentioned, compounds bearing polar functional groups, especially alcohols, have been reported to influence the organization of lecithin-stabilized interfaces by modifying molecular packing and interfacial cohesion [25–27]. In this context, isoeugenol was selected for its alcohol functionality alternative to glycerol, which may contribute to modulating interfacial structure and flexibility when combined with soy lecithin. Accordingly, in the present work, isoeugenol is incorporated primarily as co-surfactant. Additionally, it may contribute to phytosanitary activity from a conceptual perspective.

Guar gum (GG), a neutral galactomannan widely used as a thickening and stabilizing agent, is commonly incorporated into the aqueous phase of oil-in-water emulsions to increase viscosity, reduce droplet mobility, and limit coalescence [28]. Its rapid hydration in cold water and its ability to maintain nearly constant viscosity over a wide pH range (1–10) make GG particularly attractive for natural formulations [29]. As a non-ionic hydrocolloid, GG primarily provides steric stabilization without directly contributing to interfacial charge. Despite the extensive use of guar gum in conventional high-energy emulsification systems, the behavior of soy lecithin under low-energy emulsification conditions, particularly in combination with guar gum as thickening agents, and under varying pH environments, remains less explored, especially for phytosanitary formulations prepared by low-energy methods.

Currently, commercial phytosanitary products incorporate terpenes as active components at concentrations typically ranging from 5% to 10%. For example, PREVAM® PLUS contains 5–10% orange terpenes as active ingredients (with Limonene as main compound). However, such formulations often rely on synthetic additives, including alkylbenzene sulfonates and butylated hydroxytoluene, which raise concerns related to corrosivity and toxicity to aquatic ecosystems ([30]). This comparison is provided to contextualize terpene loadings and formulation strategies, rather than to imply equivalence in regulatory status or biological performance.

In this context, the present study aims to investigate the formulation of oil-in-water emulsions containing terpenes using a low-energy phase inversion method and exclusively naturally derived components. Emulsions based on R-(+)-limonene, eucalyptol, and linalool were prepared using hydrolyzed soybean lecithin as surfactant, guar gum as thickener, and isoeugenol as co-surfactant. The study adopts a systematic formulation approach to evaluate the combined effects of hydrolyzed soybean lecithin and guar gum concentration, pH of the continuous phase, and active compound polarity on the stability and microstructure of lecithin-stabilized emulsions, as well as their

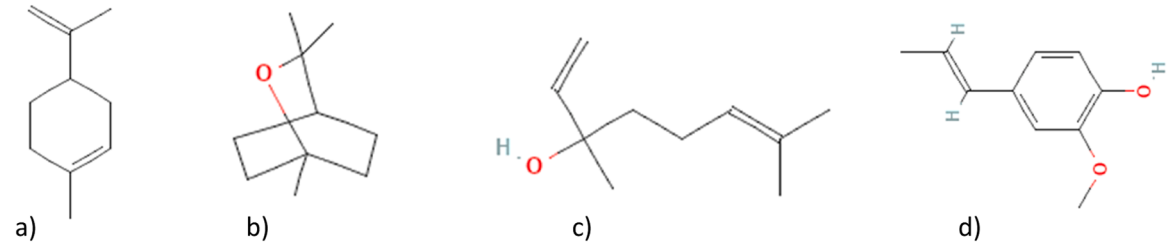

Fig. 1. Chemical 2-dimensional structure of components. R-(+)-limonene [10] (a), eucalyptol [11] (b), linalool [12] (c), and isoeugenol [13] (d) .

Table 1
Physicochemical properties of active components and co-surfactant*.

Compound	Topological Polar Surface Area (Å^2)	Partition coefficient (Log Po/w)	Hydrogen bond donor count	Hydrogen bond acceptor count	Water Solubility (mg/L at 25°C)
R-(+)-limonene	0	4.57	0	0	13.8
Eucalyptol	9.2	2.74	0	1	3500
Linalool	20.2	2.97	1	1	1590
Isoeugenol	29.5	3.04	1	2	810

*Data obtained from The National Center for Biotechnology Information database [10,11,13,12].

rheological behavior. By systematically examining these parameters within a single formulation platform, this work provides insight into the coupled effects governing the performance of lecithin-stabilized emulsions prepared by low-energy methods to encapsulate terpenes in high concentration (around 11 wt%). The results are intended to support the rational design of stable, surfactant-efficient, and fully natural terpene-based formulations, with relevance to phytosanitary formulation design.

2. Materials and methods

2.1. Materials

R-(+)-Limonene (purity 90%, mixture of enantiomers), Linalool (purity 97%) supplied by SIGMA ALDRICH, and Eucalyptol (purity 98%) supplied by FLUKA, were used as active compounds. Isoeugenol (purity 98%, mixture of cis and trans), supplied by SIGMA ALDRICH, was used as co-surfactant (Table 1). Soy lecithin with 55% hydrolysis degree (mostly L-α-phosphatidylcholine, according to product specification) (Barcitin soybean non-GMO EC) from the Barcelonesa group was used as surfactant. Guar gum from SIGMA ALDRICH was used as thickener.

2.2. Emulsion preparation

Emulsions were prepared using the low-energy emulsification and emulsion phase inversion (EPI) method employed by Ostertag et al. [14] with some modifications. Samples were prepared in a 15 mL vial under ambient conditions (approx. 23 °C).

The oil phase was prepared by mixing the corresponding amounts of thickener, surfactant, co-surfactant, and active component, followed by magnetic stirring at 700 rpm for 30 min. The aqueous phase was then added dropwise at approximately 1.4 mL/min under continuous agitation (700 rpm) until a total sample mass of 5 g was reached, and stirring was maintained for additional 60 min. The experimental design followed a two-way ANOVA model, in which the concentrations of surfactant (0.5–1.1 wt%) and thickener (0.05–0.5 wt%) were systematically varied as independent factors, while the active component and co-surfactant were kept constant at 11 wt% and 2.6 wt%, respectively. Preliminary experiments were performed to evaluate the effect of the order of phase addition, as well as the appropriate concentrations of co-surfactant and thickener, as detailed in the Supplementary Information.

Emulsion stability was evaluated through a combination of visual inspection, accelerated stress testing, and storage assessment. Immediately after preparation, samples were visually inspected to identify signs of rapid destabilization, such as phase separation or extensive creaming. All formulations were then stored at room temperature and monitored visually for up to one month, and those exhibiting instability during this period were discarded. Formulations that remained visually stable and homogeneous after one month were freshly prepared and subsequently subjected to an accelerated centrifugation test to assess their stability under stress conditions. Only the formulations showing the lowest degree of destabilization were selected for further experimental steps.

The aqueous phase of the first set of samples was prepared by acidifying deionized water with acetic acid until reaching pH 3. To study the effect of acidification of the medium on the stability and characteristics of the emulsion, the pH of the aqueous phase was modified only to those samples that remain visually stable and homogeneous after a month of preparation. The following set of samples was prepared by modifying the pH of the continuous phase to pH 5 using citric acid. Finally, the last group of samples was prepared using deionized water neutral pH. Only those samples visually stable and homogeneous after pH modifications were considered for further characterizations.

Once a stable formulation was identified, the study was extended to active components of higher polarity, namely linalool and eucalyptol, to evaluate the effect of the polarity and molecular structure of the active ingredient in the oil-water interface and the stability of the emulsion.

Samples are identified according to the active component used and the combination of surfactant (S) and thickener (GG) concentrations. For illustration, when referring to the sample with R-(+)-limonene (RL) as the active component, surfactant (S) concentration of 1.1 wt% and a thickener (G) concentration of 0.5 wt%, the code to be used will be RLS1105G.

2.3. Visual emulsion stability after preparation

After preparation, the samples were sealed with Parafilm and stored in the same preparation vial at ambient conditions (approx. 23 °C) for 24 h, to observe their evolution over time and possible phase separation. After 24 h, the emulsion stability index (ESI%) was determined by calculating the percentage of phase separation of the sample by creaming or de-oiling (Eq. 1).

$$ESI\% = \frac{Height\ of\ top\ phase}{Height\ total\ sample} \quad (1)$$

The numerator corresponds to the height of the upper phase of the sample, containing the creaming layer and/or the oil separation phase; and the denominator corresponds to the total height of the sample.

2.4. Stability under stressful conditions

After confirming visual stability of the preparations, emulsions were freshly prepared to be submitted to this assay at 24 h. Specifically, 750 µl to 500 µl were transferred to 2 mL Eppendorfs, each sample in duplicate. Samples were exposed to a stress test at a centrifugal force of 8669 RCF (relative centrifugal force) for 10 min in a Fisher AccuSpin Micro 17 centrifuge [31]. To quantify stability, the %ESI was used after centrifugation of the samples.

2.5. Optical microscopy

Freshly prepared samples of emulsions that remained visually stable and homogeneous after 24 h of preparation and showed no signs of rupture or irreversible separation after centrifugation test were analyzed, under brightfield illumination with 10x and 40x objective lenses on a Leica microscope DM1000, with a Leica ICC50 W camera attached, for image capture.

2.6. Particle size distribution

For the determination of the distribution and mean size of the

droplets generated, laser diffraction technique was applied [27,32]. The equipment used was a Mastersizer 2000 model particle analyzer with a Hydro 2000SM module for liquid dispersions (Malvern Panalytical, Malvern, Worcestershire, United Kingdom) that allows for particle/ droplet size distribution measurement within the range from 0.02 μm to 2000 μm. For the analysis, the volume of continuous medium (deionized water) was set at 100 mL. Regarding the sample volume, the necessary amount was added so that the obscuration range was between 10% and 20%. Volume distribution was characterized by the values d_{10}, d_{50}, d_{90}, and span (Eq. 2).

$$span = \frac{(d_{90} - d_{10})}{d_{50}} \quad (2)$$

Where d_{10}, d_{50} and d_{90} correspond to the sizes containing 10%, 50% and 90% of the sample volume, respectively. Span being a measure of the homogeneity and width of the size distribution.

Regarding the mean size, the De Brouckere mean diameter D[4,3] was used based also on volume distribution. Measurements were performed at 1, 3, 5, 7, 14 and 21 days after preparation. All these parameters, as well as the droplet/ particle size distribution curve, were obtained directly from the software associated with the equipment.

2.7. FT-IR spectroscopy

To evaluate the effect of continuous-phase pH on guar gum and lecithin behavior, FTIR spectra were acquired for selected aqueous systems prepared at pH 3 and pH 7. The analyzed systems included: (1) guar gum dispersions (0.5 wt%) in water, and (2) mixed dispersions containing hydrolyzed soybean lecithin (1.1 wt%) and guar gum (0.5 wt %) in water, corresponding to the concentrations used in formulation studies.

FTIR measurements were performed using an ALPHA ATR spectrometer (Bruker) operating in absorbance mode, with a spectral resolution of 4 cm^{-1} over the range 400–4000 cm^{-1} and 64 scans per spectrum. To track spectral changes associated with continuous medium pH variation, difference spectra were obtained by subtracting the spectrum recorded at pH 7 from that recorded at pH 3, allowing qualitative evaluation of pH-dependent modifications in functional group environments.

2.8. Zeta potential measurements

The zeta potential of lecithin-guar gum-isoeugenol-water mix at pH 3, 5, and 7 was analyzed with a Malvern ZSizer Advance Pro Red Label (Malvern Instruments Ltd.) at 25 ∘C. Samples were diluted 100-fold in deionized water prior to analysis, and three consecutive serial measurements were performed. The pH of the diluted samples was monitored to confirm that dilution did not substantially alter the initial pH, with an increase of approximately 0.3 units at pH 3 and 0.5 units at pH 5.

2.9. Rheological behavior

Deformation/strain and flow tests were performed on stable samples, considering the methodology used by Quintana-Martinez et al. [28] with some modifications. The analysis temperature was set at 25 ºC, with a thermal stabilization of the sample of 5 min before each test, for the samples to have the same mechanical thermal past before starting. Apparent viscosity (η) was determined from the continuous shear test performed at a shear rate between 5 s^{-1} and 1000 s^{-1}. The estimation of the viscoelastic dynamic region was evaluated with a stress sweep between 0.01 Pa and 100 Pa at a constant frequency of 1 Hz. Tests were performed on a Kinexus Pro+ rotational rheometer (Malvern Panalytical, Malvern, UK) with a parallel smooth plate geometry (20 mm diameter, 1 mm spacing), coupled to a KNX2002 C25P Peltier plate temperature control. Samples were analyzed after 24 h of preparation.

2.10. Statistical analysis

A two-way analysis of variance (ANOVA) without replication was performed using STATGRAPHICS Centurion 19 v.19.7.01 (Statgraphics Technologies, Inc., USA) to evaluate the main effects of surfactant and thickener concentrations on droplet size descriptors (D[4,3] and span) and emulsion stability (ESI%). Statistical significance (F-test) was assessed at a 95% confidence level. Effects were considered statistically significant when $p < 0.05$.

All analytical measurements were performed in triplicate for each formulation. Reported values correspond to mean values, with corresponding standard deviations.

3. Results and discussion

Despite its widespread use in phytosanitary applications as main component of orange essential oil, R-(+)-limonene lacks polar groups (Table 1), which limits its ability to engage in specific interactions with the lecithin–water interface hindering its formulation using this natural surface-active agent in a single surfactant approach. This characteristic makes a suitable model compound for investigating the addition of isoeugenol as co-surfactant and guar gum concentration as thickener on formulation stability.

Preliminary experiments showed that the order of phase addition influenced formulation stability (Figure S.1). Adding the aqueous phase into the oil phase promoted the formation of stable and homogeneous emulsions and was therefore selected for subsequent formulation trials in agreement with the works of [7] and [14]. Once this procedure was established, the effect of formulation composition was evaluated. Systems containing lecithin alone exhibited immediate oiling-off, whereas the incorporation of isoeugenol as a co-surfactant yielded stable emulsions, likely due to its moderate polarity (Table 1) and ability to interact with the oil–water interface, thanks to a moderate polar surface area of 29$Å^2$. However, creaming was observed over time, and the subsequent addition of guar gum effectively reduced creaming by increasing the viscosity of the continuous phase (Table S.1). Based on these results, the lecithin–isoeugenol –guar gum system was selected as a suitable model to systematically evaluate the effect of surfactant and thickener concentrations (from 0.5 wt% to 1.1 wt%, and 0.05 wt% to 0.50 wt% respectively) at constant co-surfactant concentration (2.6 wt%) on emulsion properties.

3.1. R-(+)-limonene formulation at pH 3

Fig. 2 shows the appearance of the emulsions after 24 h of preparation; ordered according to surfactant (0.5–1.1 wt%) and thickener (0.05–0.5 wt%) concentrations. Sample identification and their concentrations are available in Table S.2, together with the corresponding characterization results (ESI%, D[4,3], span). At the lowest gum concentration (0.05 wt%), the emulsion stability index (ESI) reached 100% for most formulations, apart from the sample containing the lowest lecithin concentration (0.50 wt%), which exhibited an ESI of 96%. This formulation showed early signs of destabilization, characterized by the formation of a thin oil layer at the top. Over time, this separation became more pronounced, especially after five days (Figure S.2). In contrast, the remaining formulations at this guar gum concentration maintained visual stability and homogeneity over the same period. Increasing the guar gum concentration to 0.20 wt% and 0.35 wt% resulted in the appearance of an additional oily upper layer (irreversible separation under storage conditions), in addition to a lower water layer (reversible separation). In this group of samples, %ESI decreased to value between 30% and 45%. Remarkably, %ESI varied with lecithin concentration. For instance, at a guar gum concentration of 0.35 wt%, %ESI improved from 46% to 80% as lecithin concentrations increased. By increasing the guar gum concentration to the highest value of 0.5 wt%, %ESI increased again to values up to 80% and 95%. In this group, only symptoms of

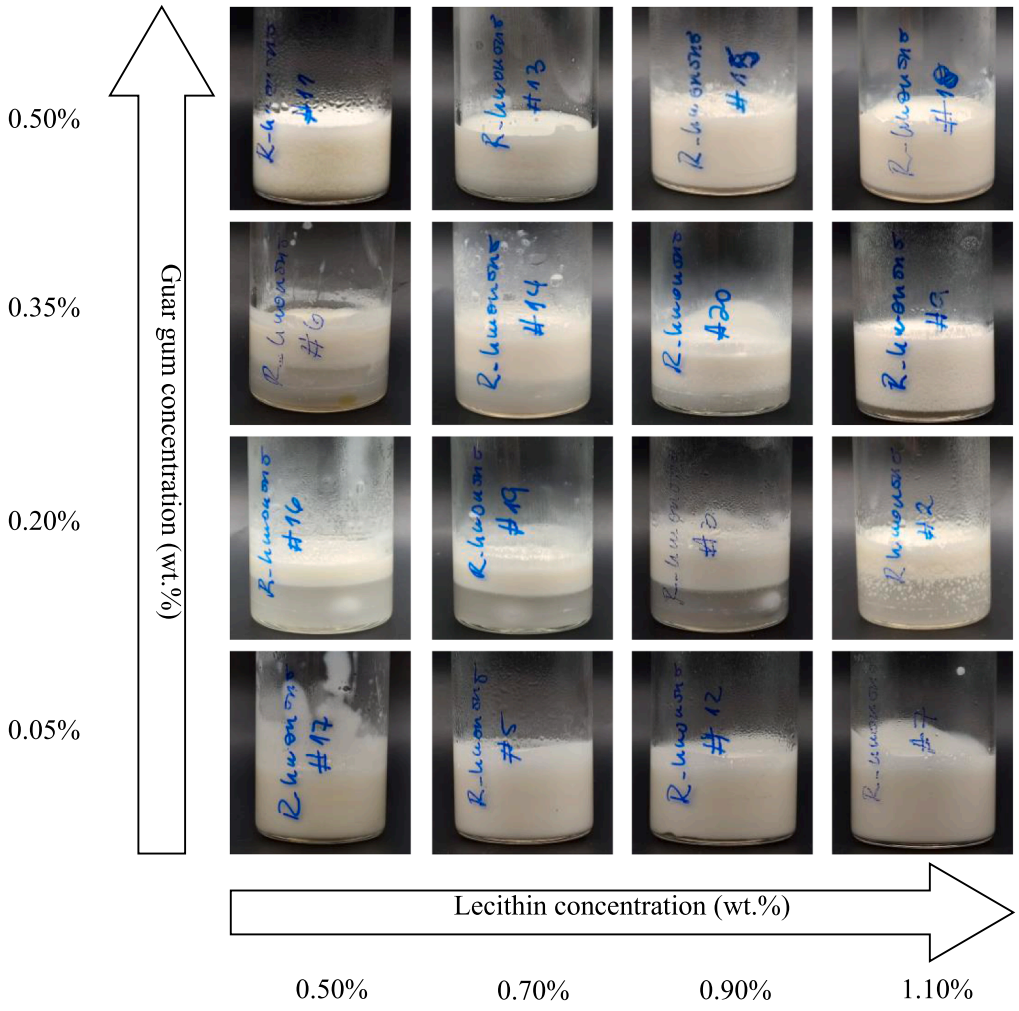

Fig. 2. Visual inspection of samples after 24 h of preparation.

reversible phase separation were detected. This phase separation persisted over time, as in the case of the sample with the lowest surfactant concentration (0.5 wt%), in which the upper creamed phase was more evident after 5 days of preparation (Figure S.2).

Polysaccharides such as xanthan or guar gum can stabilize emulsions by increasing the viscosity of the continuous phase, thereby limiting droplet mobility [18,33]. However, at low concentrations it may induce destabilization: (1) by adsorbing onto droplets and promoting flocculation through hydrogen bonding, or (2) by creating osmotic pressure gradients when unadhered [29,33]. As reported Chivero et al. [29] and Traynor et al. [18], this leads to a critical gum concentration below which aggregation increases and above which stability is restored. In this study, the authors used optical microscopy to detect the formation of droplet aggregations or flocs at thickener concentrations between

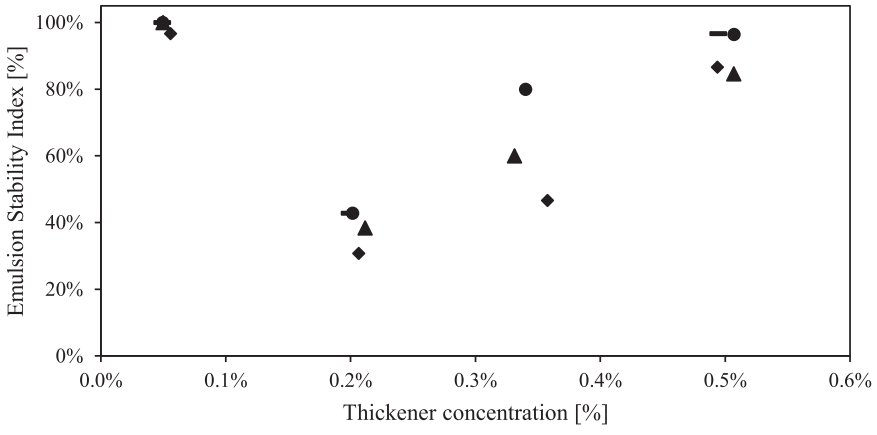

Fig. 3. Emulsion stability on guar gum, at different lecithin (surfactant) concentrations.

0.03% and 0.3%. This formation triggered reversible phase separation over time.

The relationship between guar gum concentration and emulsion stability index (ESI%) at different lecithin concentrations is shown in Fig. 3. A clear transition point was identified at approximately 0.2 wt% guar gum, representing the critical thickener concentration below which complete phase separation occurred. Beyond this threshold, increasing the guar gum content markedly improved emulsion stability. At 0.5 wt% guar gum, ESI values consistently exceeded 80% across all lecithin concentrations, and complete stabilization (100% ESI) was achieved at both the lowest and highest gum levels tested. This behavior indicates that emulsion stability in this system is governed by a balance between continuous-phase structuring and interfacial stabilization, rather than by thickener concentration alone.

Mean particle size and distribution. Fig. 4 shows the drop size distributions, according to thickener concentration. At the lowest guar gum concentration (0.05 wt%), all distributions, regardless of lecithin concentration, are unimodal, with a size D[4,3] around 100 μm and 70 μm (Table S.2). With increasing thickener concentration, the D[4,3] size shifts to values below 50 μm (Table S.2). Notably, the distribution changes from monomodal to bimodal as the lecithin concentration increases, but this change occurs at the guar gum threshold value of 0.2 wt %.

Of the unimodal group of samples (guar gum concentration 0.05 wt %), the one with the lowest D[4,3] corresponds to sample RL05S05G. This sample showed emulsion breaking and irreversible phase separation after 5 days of preparation (Figure S.2). This observation suggests that, at this concentration, guar gum alone is insufficient to fully prevent droplet interactions and coalescence over time. Furthermore, despite the formation of smaller particles, the interface formed by the lecithin in the droplets may not be strong or rigid enough to prevent their coalescence and rupture.

As the guar gum concentration increased to 0.20 wt%, the size distribution showed a well-defined bimodal behavior for all lecithin concentrations, except for the maximum concentration of 1.1 wt%. The first group of the distribution, corresponding to the smallest droplets, shows a maximum value at the lowest lecithin concentration (0.5 wt%). However, the intensity of the peak progressively decreases with increasing lecithin concentration, leading to an almost monomodal size distribution. This attenuation of the fine-droplet population is accompanied by a relative increase in the volume fraction of larger droplets. This behavior is persistent in the group of samples with the highest thickener concentration (0.50 wt%). In the case of the 0.35 wt% guar gum concentration, the distribution remains constant, practically monomodal, for all surfactant concentrations.

Huang et al. [34] studied the effect of some hydrocolloids on the droplet size distribution in canola oil emulsions. The study reported a similar bimodal behavior across all the hydrocolloids analyzed, including xanthan, acacia, and guar gums, at concentrations comparable to those used in the present study (0.05–0.50 wt%). The author points out the thickening effect of these polysaccharides. Specifically, they noted that as the concentration of polysaccharides in the medium increased, the homogenization efficiency decreased, resulting in a shift from smaller to larger particle groups and, consequently, an increase in droplet size. Comparing the behavior observed by Huang et al. [34] with the samples of the present study, the shift of the bi-modal distributions to monomodal trending distributions could be attributed to a combined effect between surfactant and thickener.

At both low (0.5 wt%) and high (1.1 wt%) surfactant concentrations, similar trends were observed in the evolution of droplet size

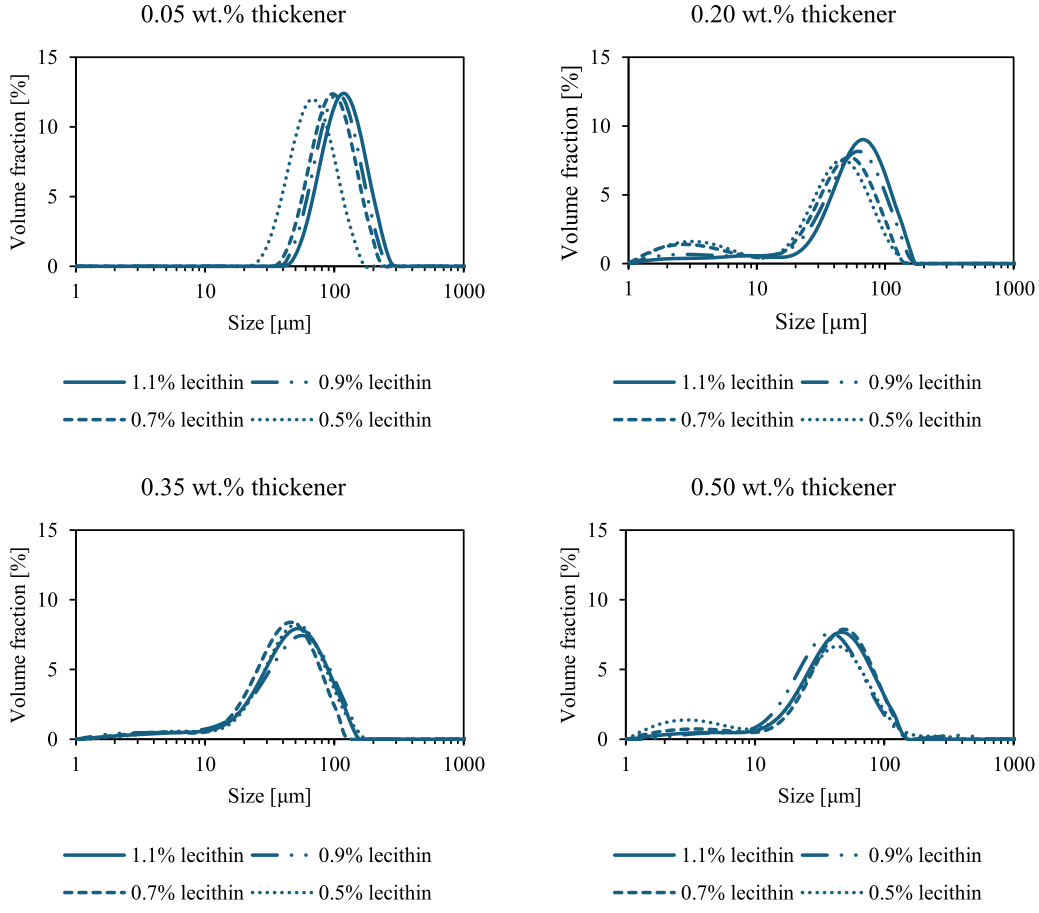

Fig. 4. Particle size distribution according to thickener and lecithin concentrations.

distributions as a function of guar gum content (Figure S.3). In all cases, increasing the thickener concentration led to a decrease in the average droplet size (D[4,3]), confirming the stabilizing effect of guar gum through modification of the continuous-phase properties. However, droplet size distributions did not always become fully homogeneous, and bimodal profiles could persist at intermediate thickener concentrations, indicating limitations in droplet homogenization beyond the critical thickener concentration. These features are consistent with previous reports on hydrocolloid-stabilized oil-in-water emulsions, where increased polysaccharide content may hinder homogenization efficiency and promote the coexistence of distinct droplet populations [34].

The evolution over time of D[4,3] and span was monitored for samples containing 0.05 wt% thickener and surfactant concentrations of 0.7 wt%, 0.9 wt%, and 1.1 wt%. These were the only formulations that maintained visual homogeneity and physical stability over a 28-day period (Figure S.4). Initially, a difference in size is observed that is directly proportional to the amount of surfactant. With time, the size D[4,3] evolves and increases for all samples, suggesting interactions between the droplets, causing the increase in size. In the concentration range studied, with the progressive increase of the surfactant concentration it was detected that the average size tends to reach a constant value. Proof of this is that, after 21 days of storage, samples RL09S05G and RL11S05G reach a similar average size, despite having different surfactant concentrations.

Regarding the homogeneity of the distribution (span), all samples maintain a constant distribution over time, regardless of the increase in the mean size. However, the sample with the highest surfactant concentration (RL11S05G) begins to modify its distribution after 21 days of storage, even though having an almost constant mean size around 120 μm. When observing the particle size distribution after 28 days (Figure S.5), particles of size between 1 μm and 40 μm start to appear. This new distribution could indicate a process of partial emulsion breakdown over time. In the sample with intermediate surfactant concentration RL09S05G, this behavior seems to occur, though it is less pronounced.

A two-factor ANOVA (Table S.3) without replications was used to evaluate the relative contribution of surfactant and thickener concentrations to the variability of D[4,3], span, and ESI%. The overall ANOVA model for D[4,3] was statistically significant ($F = 12.31$, $p = 0.001$). Type III sums of squares revealed that thickener concentration was the dominant factor ($p = 0.0003$), while the effect of surfactant concentration was not statistically significant ($p = 0.13$). For the span, the overall ANOVA model was statistically significant ($F = 9.92$, $p = 0.0024$). Type III sums of squares showed that thickener concentration had a strong and statistically significant effect ($p = 0.0007$), whereas surfactant concentration was not significant ($p = 0.27$). The consistent dominance of thickener concentration over both D[4,3] and span indicates that the rheological modification of the continuous phase governs droplet size distribution under the investigated conditions. For the emulsion stability index (ESI), the overall ANOVA model was not statistically significant ($F = 0.48$, $p = 0.63$), and neither surfactant nor thickener concentration showed a significant effect ($p > 0.05$). The lack of statistically significant differences in ESI may be related to the semiqualitative character of this parameter, since it does not differentiate between distinct destabilization phenomena (e.g., reversible or irreversible). Additionally, it suggests that macroscopic emulsion stability can be governed by additional mechanisms.

Stability under stressful conditions and rheological behavior. As the only ones that were visually homogeneous and stable after 1 month of storage, the samples with the lowest thickener concentration (0.05 wt%) and surfactant concentrations between 0.7 wt% to 1.1 wt% were freshly prepared and exposed to stress stability analysis 24 h after: RL07S05G, RL09S05G, and RL11S05G (Figure S.6). All three samples exhibited a thin oil layer on the surface after centrifugation. However, the extent of phase separation decreased with increasing lecithin concentration, accounting for approximately 15% of the total sample volume at the lowest surfactant level, 11% at the intermediate concentration, and 10% at the highest concentration. Notably, the formulation with the highest lecithin content showed the lowest degree of irreversible phase separation, despite presenting the largest average droplet size and the most pronounced temporal increase in D[4,3] and span (Figure S.4).

Rheological characterization further supports these observations (Fig. 5). Formulation RL11S05G exhibits the highest apparent viscosity at low shear rates, consistent with its improved resistance to stress-induced destabilization. Although differences in mean droplet size among the three samples are relatively small (around 8 μm, Figure S.4), increasing lecithin concentration appears to enhance the macroscopic resistance of the system to flow and separation. This behavior is consistent with literature reports indicating that lecithin-rich interfaces can exhibit increased viscoelastic character as surfactant concentration increases [20]. Previous studies have attributed such behavior to the accumulation of lecithin molecules at the oil–water interface, forming interfacial structures reinforced by hydrogen-bonding interactions between phospholipid headgroups [20,35]. The observed increase in apparent viscosity and resistance to mechanical stress is consistent with this interpretation.

Moreover, and with respect to the presence of guar gum as a thickener, Quintana-Martinez et al. [28] studied the effect of the guar gum-lecithin combination on the rheological behavior of oil-in-water formulations of sunflower oil. In their study, the authors concluded that the effect of the thickener has greater influence on the apparent viscosity and the plastic-elastic regions of the formulations than surfactant concentration. They demonstrated that, in lecithin–guar gum systems, thickener concentration predominantly governs apparent viscosity and viscoelastic behavior at guar gum contents around 0.5–1 wt %. In the present study, the guar gum concentration (0.05 wt%) is at least one order of magnitude lower than those reported values. Accordingly, the observed rheological differences are less pronounced, but an increase in apparent viscosity with increasing surfactant concentration is still evident. This suggests that, at low guar gum levels, surfactant–thickener and surfactant–water interactions contribute to macroscopic stability without inducing gel-like behavior.

In the stress-strain test (Fig. 5), the samples display a clear two-region response. In the linear viscoelastic region, the storage modulus ($G' \sim 10^2$ Pa) exceeds the loss modulus (G'') by nearly two orders of magnitude, indicative of a well-connected, gel-like network under small deformations [36]. Once the critical stress is surpassed (around 2 Pa for RL07S05G, and around 10 Pa for RL09S05G and RL11S05G), G' declines while G'' displays a weak local maximum (stress overshoot), a response widely associated with the resistance of the long and complex hydrocolloid chains when reaching a critical deformation stress, typical yielding transitions observed in structured fluids such as complex hydrocolloids polymer solutions and soft colloidal gels [37,38]. This overshoot can be interpreted as temporary resistance of the network to deformation, followed by reorganization or partial breakdown of chain associations. The modest magnitude of the overshoot suggests that the guar gum network is sufficiently structured to provide resistance, but also flexible enough to rapidly rearrange once deformation progresses.

Overall, although the limonene-based formulations at pH 3 remain visually stable over extended storage, their limited resistance to mechanical stress indicates that further optimization is required. To enhance resistance to such stress-induced destabilization, increasing the lecithin concentration would be a logical strategy. Prior studies have found that exceeding a certain lecithin concentration leads to an increase in viscosity, promoting gel formation due to interaction of the lecithin with polar solvents like water [39]. Consequently, rather than further increasing surfactant or thickener content, the next step of this study focuses on evaluating the influence of the pH of the continuous phase on formulation stability, using the most resistant formulation in the previous centrifugation assay RL11S05G (1.1 wt% surfactant and 0.05 wt% thickener) as the reference system.

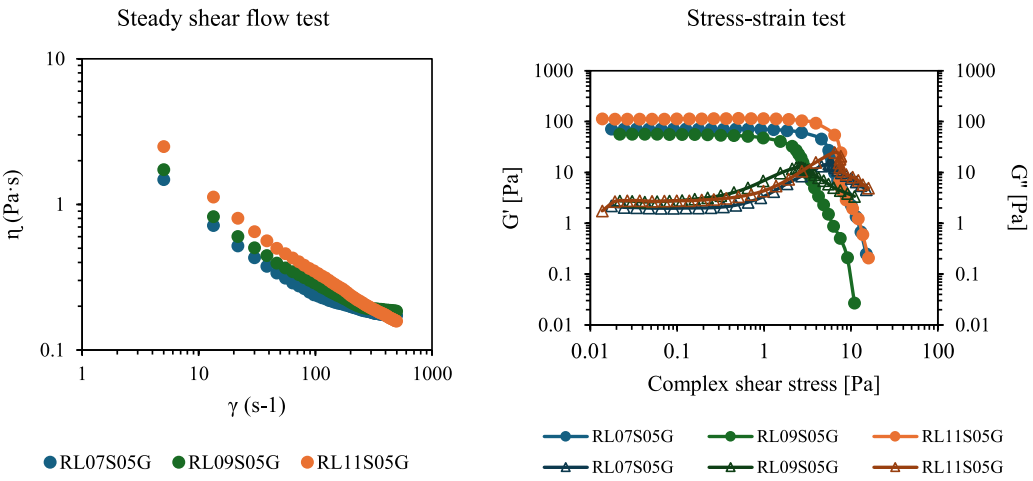

Fig. 5. Rheological tests of visually stable and homogeneous samples.

3.2. *R-(+)-limonene formulation at pH 3, pH 5, and pH 7*

To observe the influence of the acidity of the continuous medium on the stability of the sample, the pH of the formulation was shifted to pH 5 and pH 7. After 24 h of preparation, the samples showed visual apparent homogeneity and stability percentages of 100%.

Mean particle size and distribution. Like pH 3 sample, pH 5 and pH 7 samples presented a unimodal and narrow distribution, maintaining a span around 0.97. However, the D[4,3] sizes turned out to be up to 15% larger than that of the pH 3 sample (Figure S.7 and Table S.4).

This slight variation in droplet size and distribution (around 8 μm deviation from the mean) may be attributed to the influence of pH on the behavior of both thickener and surfactant. Regarding the thickener, acidification of the medium has been reported to affect the hydrogen-bonding capacity of galactomannan-based polysaccharides, which may weaken polysaccharide–water interactions and reduce thickening efficiency. Wang et al. [40] investigated the behavior of guar-gum dispersions under acidic conditions (pH 1–6.5) and moderate temperatures (25–50 °C), reporting that the polysaccharide structure remains essentially intact at pH values equal to or above 3. In addition to the chemical stability, the authors detected a moderate reduction in viscosity under acidic conditions. This behavior was attributed to changes in the hydrogen-bonding environment of the system. When proton concentration increases, water structure and intermolecular interactions between galactomannan chains and between galactomannan and water molecules may suffer alterations, thereby reducing thickening efficiency without compromising the chemical stability of the guar-gum network [40]. This interpretation is further supported by FTIR analysis of guar-gum aqueous dispersions and guar gum-lecithin system at pH 3 and pH 7 (Fig. 6). The differential spectra of guar gum dispersion revealed a subtle change in the O–H stretching region (3000–3600 cm^{-1}), characterized by a redistribution of intensity, including a negative contribution around 3200–3300 cm^{-1}. Such behavior is consistent with pH-induced reduction in hydrogen-bonding networks, related to pH media acidification from pH 7 to pH 3. No new bands attributable to polysaccharide backbone degradation were detected. These observations indicate that acidification primarily affects the hydrogen-bonding environment rather than inducing chemical modification of the

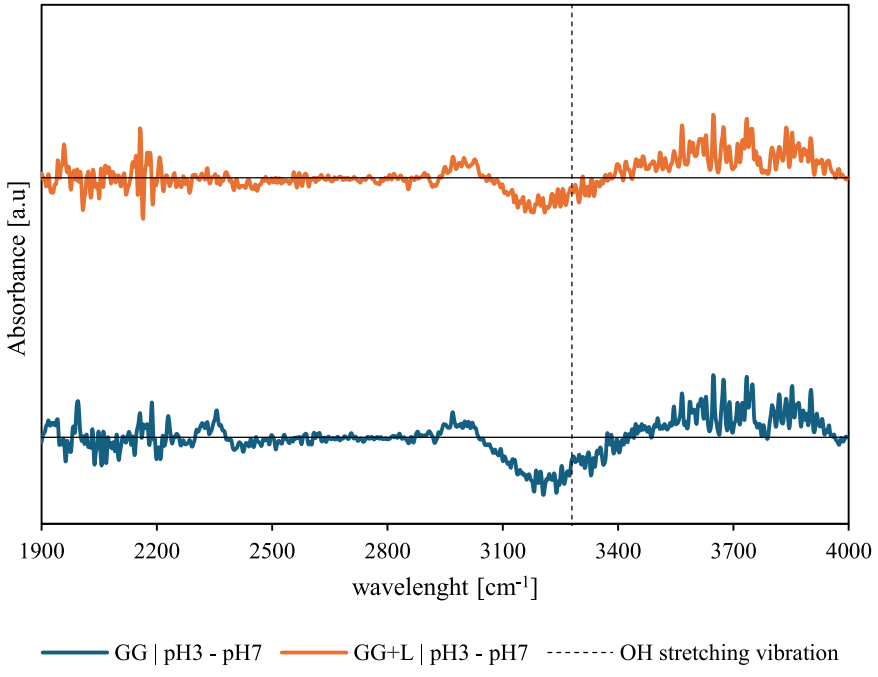

Fig. 6. FTIR difference spectra (pH 3 – pH 7) of guar gum and guar gum–lecithin aqueous dispersions.

polysaccharide structure.

Moving to lecithin, several authors have evaluated the effect of pH on its surfactant performance. Östbring et al. [41] reported that acidification shifted the zeta potential toward less negative values, while simultaneously decreasing the average droplet size. In contrast, Nash & Erk [20] observed that lowering the pH led to more negative zeta potential values, and an increase in droplet size. Despite these differing trends, both studies clearly demonstrate that the pH of the medium significantly influences the interfacial behavior of lecithin-based systems. Under the conditions of the present study, when including lecithin in the system, differential FTIR spectra revealed an improvement in the O–H stretching region (3100–3600 cm^{-1}), indicating pH-dependent restructuring of hydrogen bonding networks (Fig. 6). Notably, the negative peak exhibited a lower intensity and a different profile in guar gum–lecithin systems compared to guar gum alone, suggesting that the presence of lecithin modulates hydroxyl-associated hydrogen bonding under acidic conditions. These spectral variations are consistent with acid-induced modification of hydroxyl hydrogen-bonding environment. Although FTIR does not allow direct quantification of protonation, these spectral changes support the view that acidification alters the local chemical environment of both polysaccharide and phospholipid.

Examination of the zeta potential trends for the present lecithin–guar-gum–isoeugenol–water system (Fig. 7) shows a progressive increase in negative surface charge from emulsions initially prepared at acidic conditions to those prepared at neutral pH (from −49 mV at pH 3 to −65 mV when analyzing neutral sample). This trend is consistent with the observations reported by Östbring et al. [41], who also described less negative zeta potential values and a slight increase in mean droplet size under acidic conditions in lecithin-stabilized systems. These values reflect the electrokinetic behavior of the system under the measurement conditions and suggest that pH-dependent interactions modulate surface charge development.

Overall, the results suggest that droplet formation and stability are therefore governed by the interactions between surfactant behavior, thickener performance, and the pH of the aqueous medium, rather than by a single dominant mechanism.

Stability under stressful conditions and rheological behavior. When the samples were exposed to the stress stability test, the variation in pH did not seem to provide any notable improvement to the stability of the sample (Figure S.8). Although phase separation is less pronounced for pH 5 and 7 than for pH 3 sample, a translucent layer at the top of the formulation, corresponding to the separated oil phase, can be observed in all samples.

A slight increase in apparent viscosity was recorded with increasing pH in the low shear rate region when performing the steady shear flow test (Fig. 8), as expected according to Wang et al. [40]. On the other hand, although the pH 5 and pH 7 samples showed no difference from each other, they did show a separation from the pH 3 sample as the shear rate increased. This indicates a slight effect of pH on sample viscosity and stability. This trend is most evident in the deformation stress strain test (Fig. 8). The difference between the storage modulus (G′) and loss modulus (G″) increases as the pH of the formulation shifts toward higher values. At pH 3, G′ values are around 100 Pa, whereas at pH 5 and pH 7 they increase to approximately 200 Pa, while G″ remains comparatively low, in the range of 4–5 Pa across all pH conditions. In addition, once the critical strain is exceeded, G″ displays a stress overshoot whose magnitude increases with pH neutralization, reaching maximum values when complex shear stress reaches 10 Pa of complex shear stress, which is indicative of enhanced resistance of the structured network to deformation. This widening gap between G′ and G″, together with the increase in overshoot magnitude, indicates that intermolecular interactions such as hydrogen bonding are strengthened under less acidic conditions.

Although acidification appears to favor short-term droplet formation, pH-dependent modifications of surfactant and thickener interactions reduce viscosity and limit resistance to mechanical stress at low pH. Since no substantial differences were observed between pH 5 and pH 7, subsequent experiments focused on increasing thickener concentration under neutral conditions to further enhance formulation stability.

3.3. *R-(+)-limonene formulation at pH 7 and varying concentration of thickener*

After sample preparation, 100% of ESI% was detected when increasing the concentration of guar gum from 0.05 to 0.50 wt% at pH 7, resulting in a considerable improvement in the stability of the sample. Reaffirming the idea reported by [20,40], that intermolecular thickener-surfactant-water interactions can be affected not only by concentration of these, but also by the pH of the medium.

Mean particle size and distribution. Fig. 9 shows the size distribution when increasing thickener concentration. Alongside the unimodal behavior observed in the three samples, the graph highlights two key effects related to their polydispersity: (1) the influence of neutral pH on the ability of the surfactant–thickener system to generate smaller and more uniformly distributed droplets (Table S.5), and (2) the impact of increasing thickener concentration on the homogenization and dispersion of these droplets.

In agreement with previous results, increasing thickener content promotes emulsion stability by strengthening the continuous phase and limiting droplet mobility, rather than by direct adsorption at the

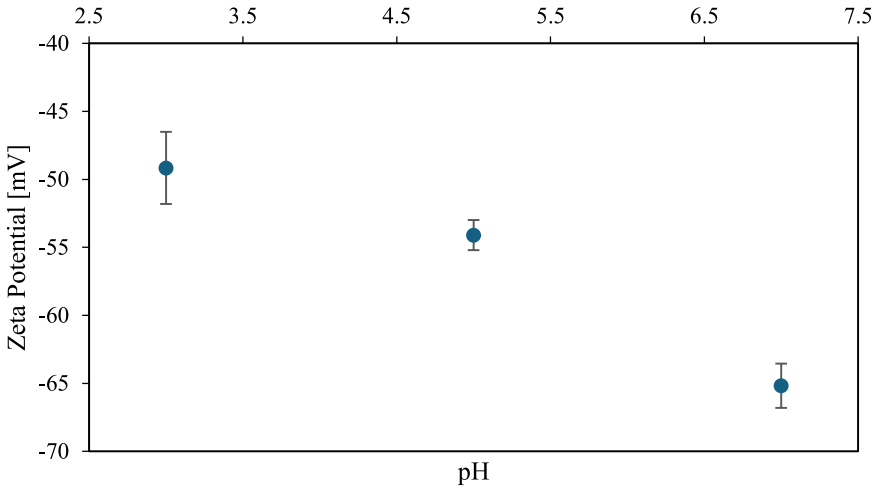

Fig. 7. Aqueous phase pH influence on zeta potential of lecithin–guar-gum–isoeugenol–water system.

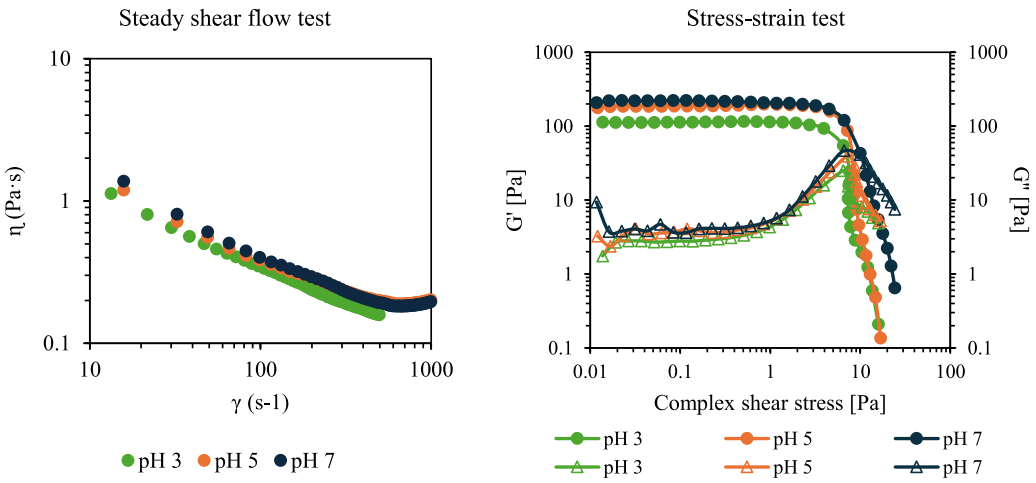

Fig. 8. Rheological tests of samples RL11S05G at pH 3, 5, and 7.

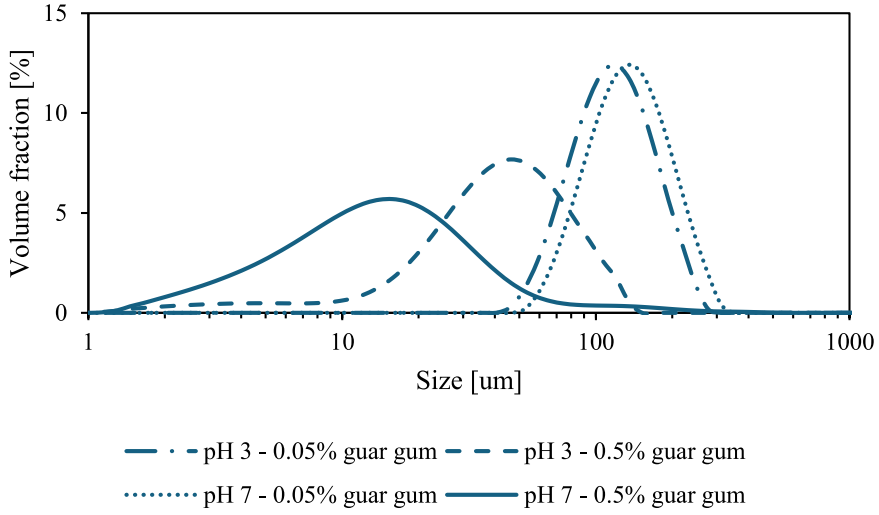

Fig. 9. Particle size distribution at constant lecithin concentration (1.1%) - pH and thickener concentration variation.

oil–water interface. Under neutral conditions, the guar gum network appears to retain its thickening efficiency, favoring reduced droplet mobility and improved resistance to coalescence. These observations agree with previous reports showing that acidic conditions weaken hydrogen-bonding interactions in polysaccharide–water systems, while less acidic environments promote stronger intermolecular associations and higher effective viscosity [40]. This interpretation is further supported by the pH-dependent changes observed in the O–H stretching region of the FTIR spectra (Fig. 6).

Stability under stressful conditions and rheological behavior. The new

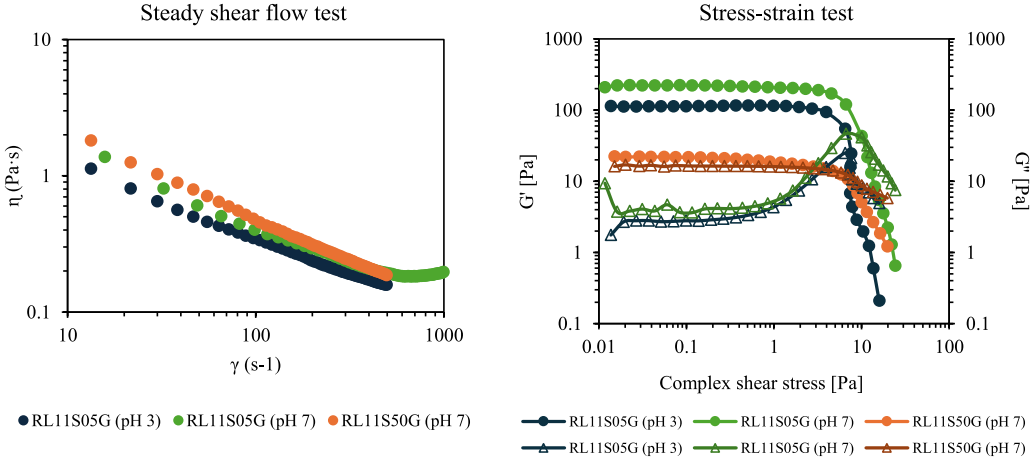

Fig. 10. Rheological test for pH and thickener concentration comparison.

sample was submitted to the stability test, as were the previous formulations. It was observed that increasing the thickener concentration at neutral pH enhanced the stability of the formulation and enabled it to withstand the stress-stability test without irreversible phase separation or rupture (Figure S.9).

When observing the behavior of the sample in the flow test (Fig. 10) and comparing it with the response of the samples with lower thickener content (0.05 wt%) at pH 3 or 7, the apparent viscosity of the sample appears to have increased slightly at low shear rates, which could be due to the effect of the increased thickener concentration. As the shear rate increases, however, neutral pH samples appear to behave similarly. In the stress strain test (Fig. 10), significant differences were observed between the two deformation zones. In the linear viscoelastic region, the gap between the storage modulus (G′) and the loss modulus (G″) is considerably reduced in the modified formulation. Although G′ remains higher than G″, both moduli are of the same order of magnitude (around 20 Pa), the reduced separation between them suggests that the formation of a strong gel-like network is slowed down. A second notable difference is observed in the transition zone, where the weak stress overshoot phenomenon is no longer detected. This behavior indicates that increasing the guar gum concentration promotes stronger thickener–surfactant and thickener–water interactions, which reduce the resistance of galactomannan chains to deformation. This observation is consistent with the behavior reported by Quintana-Martinez et al. [28], who showed that although soy lecithin does not significantly increase viscosity in mixed systems, it interacts with polysaccharide chains in a way that influences the breaking and reformation of intermolecular bonds.

3.4. R-(+)-limonene, eucalyptol and linalool formulation at pH 7

Based on previous results, the formulation conditions were fixed at pH 7, 1.1 wt% surfactant, and 0.5 wt% thickener. Under these conditions, the system was further evaluated for the encapsulation of different volatile active compounds, eucalyptol (EU) and linalool (LNL), using R-(+)-limonene as a reference. This approach allowed assessment of how variations in molecular features influence emulsion behavior under identical formulation parameters. These compounds were selected for their difference in structure and polarity (Table 1) such as number of groups capable of forming/accepting hydrogen bonding (both with 1), and topological polar surface area (20.2 $Å^2$ and 9.2 $Å^2$ respectively), versus the totally non-polar R-(+)-limonene. As shown in Fig. 11, after 24 h of preparation, all samples showed both homogeneity and visual stability of 100%.

Mean particle size and distribution. Fig. 12 shows the droplet size distribution of the samples after 24 h of preparation. R-(+)-limonene (D[4,3]: 19.6 ± 0.6 μm), and eucalyptol (D[4,3]: 51.9 ± 0.2 μm) formulations show unimodal distributions; however, the distribution corresponding to the eucalyptol formulation presents is narrower (span: 1.336 ± 0.004), and an almost symmetric compared to that of R-(+)-limonene (span: 2.51 ± 0.04).

The linalool sample exhibits a bimodal droplet size distribution (D[4,3] = 67.6 ± 0.4 μm), with two distinct populations centered at approximately 2 μm (about 30% of the cumulative volume) and 100 μm (about 70%). Compared to the less polar R-(+)-limonene system, which forms smaller and more uniformly distributed droplets, linalool leads to larger droplets and bimodal behavior. This difference can be attributed to higher polar surface area of linalool and presence of both hydrogen bond donors and acceptors, which may promote partial interactions with the aqueous phase and the interfacial layer, thereby altering interfacial organization and droplet dynamics.

Optical microscopy provided additional insight into these effects (Fig. 12). The eucalyptol formulation (Fig. 12.B) exhibited smaller droplets but displayed regions of interstitial continuous phase, suggesting partial aggregation of droplet clusters. The R-(+)-limonene sample (Fig. 12.A) showed a more uniformly packed distribution, with fewer visible aggregates. The linalool formulation (Fig. 12.C) was particularly distinctive: despite its bimodal distribution in laser diffraction, the micrograph revealed densely packed droplets with no visible interstitial voids and an overall smaller apparent droplet size compared with the less polar compounds. This behavior likely reflects the coexistence of small, well-dispersed droplets and larger structures associated with localized organization within the continuous phase, consistent with mechanisms previously proposed for polysaccharide-containing emulsions [34].

Stability under stressful conditions and rheological behavior. All formulations remained visually intact during the centrifugation test, with no detectable signs of instability (oil separation or creaming) (Figure S.10).

The flow curves (Fig. 13) show a similar qualitative behavior for all formulations; however, clear differences arise in the absolute viscosity values. As the polarity of the active compound decreases, the curves shift toward higher apparent viscosities. The linalool-based emulsion, which exhibited a bimodal droplet size distribution, showed the lowest apparent viscosity.

The relatively low viscosity of the linalool-based emulsion indicates that the larger structures observed in its bimodal droplet size distribution do not correspond to thickener-derived aggregates capable of imparting gel-like behavior. Instead, they are likely associated with weakly interacting droplet populations that coexist without significantly contributing to the bulk rheological response. This interpretation is supported by stress strain tests (Fig. 13), which show an almost negligible gap between the storage (G′) and loss (G″) moduli for all three formulations, confirming that none of the systems exhibit gel-like characteristics. In addition, the linalool formulation exhibits the lowest transition point between G′ and G″, indicating a reduced resistance to deformation. The observed increase in transition values with decreasing terpene polarity further confirms that, beyond the

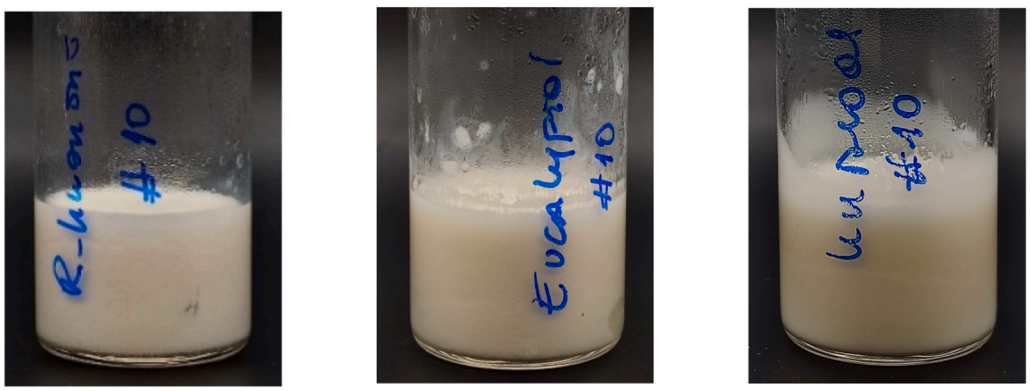

Fig. 11. Visual inspection of formulations with different active components after 24 h of preparation: R-(+)-limonene (left), eucalyptol (middle), and linalool (right).

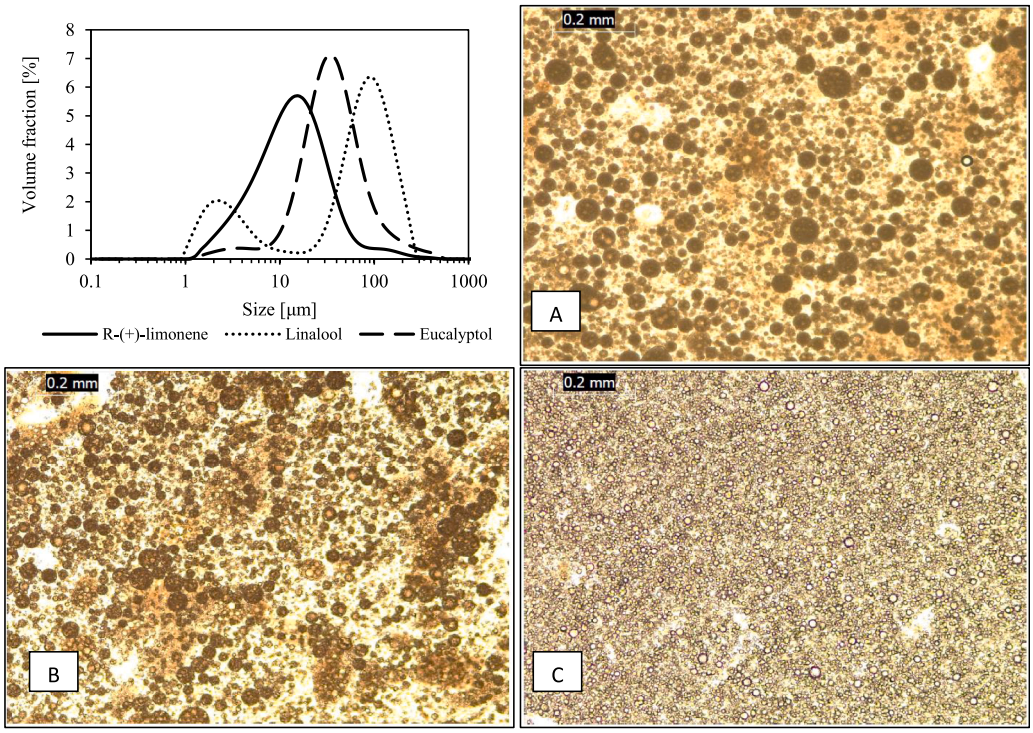

Fig. 12. Particle size distribution and micrographs of formulation for different active components: R-(+)-limonene (A), eucalyptol (B), and linalool (C).

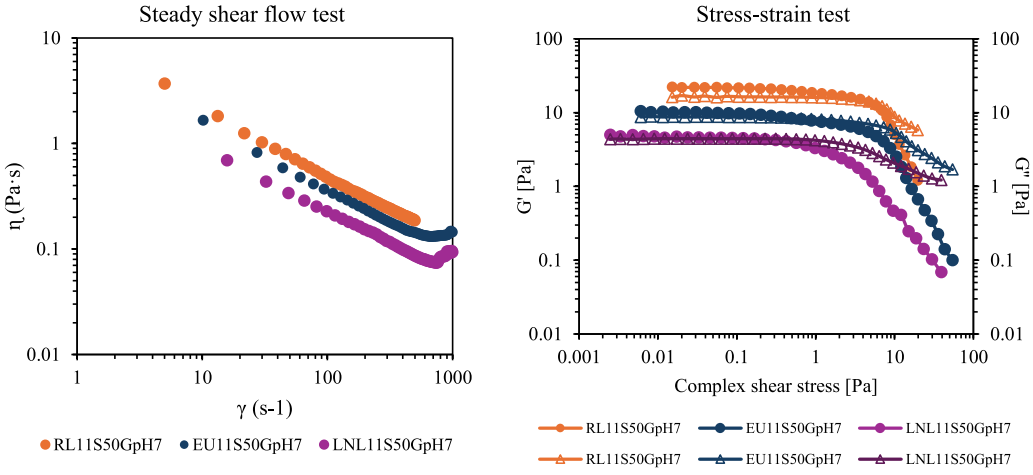

Fig. 13. Rheological test of different active component formulations: R-(+)-limonene (RL), eucalyptol (EU), and linalool (LNL).

surfactant–thickener–co-adjuvant system, the physicochemical properties of the active compound play an important role in determining droplet organization and rheological response in oil-in-water emulsions, in agreement with previous reports on terpene-containing systems [27].

4. Conclusion

This work demonstrates that the stability and microstructure of terpene-based oil-in-water emulsions prepared by low-energy phase inversion are governed by the combined effects of surfactant concentration, thickener concentration, continuous-phase pH, and active compound polar or nonpolar character. Using exclusively naturally derived components, hydrolyzed soybean lecithin, guar gum, and isoeugenol, stable formulations containing 11 wt% terpene were successfully obtained. In this formulation strategy, isoeugenol was incorporated as a co-surfactant based on its molecular structure, since the presence of the phenolic hydroxyl group gives it a moderate polar character that may facilitate interactions within the phospholipid-stabilized oil-water interface.

For the apolar terpene R-(+)-limonene, neutral pH conditions and appropriate lecithin guar-gum concentrations (1.1 wt% and 0.5% wt., respectively) yielded stable emulsions with a unimodal droplet size distribution. Acidification of continuous phase modified surface charge development and rheological response, leading to reduced stability, as supported by zeta potential trends, rheological measurements, and complementary FTIR analysis of pH-dependent hydrogen-bonding settings.

Extension of the formulation matrix to more polar terpenes (eucalyptol and linalool) revealed that active compound polarity significantly influences droplet organization and rheological behavior, even under identical formulation conditions. Eucalyptol-based systems remained stable with wider size distributions, whereas linalool-based emulsions

showed bimodal profiles, consistent with their higher polarity. These findings highlight that emulsion performance in lecithin-stabilized systems cannot be interpreted solely in terms of surfactant or thickener concentration but must consider polarity-driven interactions within the interfacial and bulk phases. Overall, this study provides a systematic experimental framework for the rational design of fully natural, low-energy terpene emulsions (with concentrations of active component around 11 wt%), and clarifies the respective roles of formulation composition, medium pH, and active compound physicochemical properties in determining stability.

Ongoing work focuses on assessing formulation performance under application-relevant conditions, including active ingredient retention and interactions with target surfaces, to better understand how surface–formulation dynamics affect delivery efficiency and volatilization control.

CRediT authorship contribution statement

Soraya Rodríguez-Rojo: Writing – review & editing, Supervision, Conceptualization. **Andrea Casas González:** Writing – original draft, Investigation, Data curation, Conceptualization.

Declaration of Generative AI and AI-assisted technologies in the manuscript preparation process

During the preparation of this work the authors used OpenAI's ChatGPT models 4o, 5, and 5.1 for literature searching, language editing and writing refinement. After using this tool, the authors reviewed and edited the content as needed and takes full responsibility for the content of the published article.

Declaration of Competing Interest

The authors declare that they have no known competing financial interests or personal relationships that could have appeared to influence the work reported in this paper

Acknowledgements

Financial support of the Department of Education of the Junta de Castilla y León and FEDER Funds (CLU-2025-2-05) is gratefully acknowledged by the authors. The authors would also like to acknowledge the support of the ProCerealTech group at the University of Valladolid, especially PhD. Marina Villanueva, for providing access to analytical equipment and support in rheological analyses.

Appendix A. Supporting information

Supplementary data associated with this article can be found in the online version at doi:10.1016/j.colsurfa.2026.140209.

Data Availability

Data will be made available on request.

References

[1] Food and Agriculture Organization of the United Nations. (n.d.). Sustainable Management. Global Action for Fall Armyworm Control. Retrieved ⟨https://www.fao.org/fall-armyworm/sustainablemanagement/en/⟩.
[2] V. Ninkuu, L. Zhang, J. Yan, Z. Fu, T. Yang, H. Zeng, Biochemistry of terpenes and recent advances in plant protection, Int. J. Mol. Sci. 22 (11) (2021), https://doi.org/10.3390/ijms22115710.
[3] Parlamento Europeo, Directiva 2009/128/Ce, D. Of. De. La UnióN. Eur. (2009) 71–86.
[4] M. Hyldgaard, T. Mygind, R. Piotrowska, M. Foss, R.L. Meyer, Isoeugenol has a non-disruptive detergent-like mechanism of action, Front. Microbiol. 6 (JUL) (2015) 1–14, https://doi.org/10.3389/fmicb.2015.00754.
[5] M. Zaker, Natural Plant Products as Eco-friendly Fungicides for Plant Diseases Control- A Review, Agriculturists 14 (1) (2016) 134–141, https://doi.org/10.3329/agric.v14i1.29111.
[6] EU Pesticides Database - Active substances. (n.d.). Retrieved November 24, 2025, from ⟨https://ec.europa.eu/food/plant/pesticides/eu-pesticides-database/start/screen/active-substances⟩.
[7] J. Feng, R. Wang, Z. Chen, S. Zhang, S. Yuan, H. Cao, S.M. Jafari, W. Yang, Formulation optimization of D-limonene-loaded nanoemulsions as a natural and efficient biopesticide, Colloids Surf. A Physicochem. Eng. Asp. 596 (January) (2020) 124746, https://doi.org/10.1016/j.colsurfa.2020.124746.
[8] M.D. Lopez, A. Maudhuit, M.J. Pascual-Villalobos, D. Poncelet, Development of formulations to improve the controlled-release of linalool to be applied as an insecticide, J. Agric. Food Chem. 60 (5) (2012) 1187–1192, https://doi.org/10.1021/jf204242x.
[9] T.N. Barradas, K.G. de Holanda e Silva, Nanoemulsions of essential oils to improve solubility, stability and permeability: a review, Environ. Chem. Lett. 19 (2) (2021) 1153–1171, https://doi.org/10.1007/s10311-020-01142-2.
[10] (+)-Limonene | C10H16 | CID 440917 - PubChem. (n.d.). Retrieved November 25, 2025, from ⟨https://pubchem.ncbi.nlm.nih.gov/compound/440917⟩.
[11] 1,8-Cineole | C10H18O | CID 2758 - PubChem. (n.d.). Retrieved November 25, 2025, from ⟨https://pubchem.ncbi.nlm.nih.gov/compound/2758⟩.
[12] Linalool | C10H18O | CID 6549 - PubChem. (n.d.). Retrieved November 25, 2025, from ⟨https://pubchem.ncbi.nlm.nih.gov/compound/6549⟩.
[13] Isoeugenol | C10H12O2 | CID 853433 - PubChem. (n.d.). Retrieved November 25, 2025, from ⟨https://pubchem.ncbi.nlm.nih.gov/compound/Isoeugenol⟩.
[14] F. Ostertag, J. Weiss, D.J. McClements, Low-energy formation of edible nanoemulsions: Factors influencing droplet size produced by emulsion phase inversion, J. Colloid Interface Sci. 388 (1) (2012) 95–102, https://doi.org/10.1016/j.jcis.2012.07.089.
[15] T.D.T. Vinh, L.T.M. Hien, D.T.A. Dao, Formulation of black pepper (Piper nigrum L.) essential oil nano-emulsion via phase inversion temperature method, Food Sci. Nutr. 8 (4) (2020) 1741–1752, https://doi.org/10.1002/fsn3.1422.
[16] Harasym, J., & Banaś, K. (2024). Lecithin's Roles in Oleogelation. In Gels (Vol. 10, Number 3). Multidisciplinary Digital Publishing Institute (MDPI). ⟨https://doi.org/10.3390/gels10030169⟩.
[17] C.R. Scholfield, Composition of soybean lecithin, J. Am. Oil Chem. Soc. 58 (10) (1981) 889–892, https://doi.org/10.1007/BF02659652.
[18] M.P. Traynor, R. Burke, J.M. Frías, E. Gaston, C. Barry-Ryan, Formation and stability of an oil in water emulsion containing lecithin, xanthan gum and sunflower oil, Int. Food Res. J. 20 (5) (2013) 2173–2181.
[19] A.M. Aura, P. Forssell, A. Mustranta, T. Suortti, K. Poutanen, Enzymatic hydrolysis of oat and soya lecithin: Effects on functional properties, J. Am. Oil Chem. ' Soc. 71 (8) (1994) 887–891, https://doi.org/10.1007/BF02540468.
[20] J.J. Nash, K.A. Erk, Stability and interfacial viscoelasticity of oil-water nanoemulsions stabilized by soy lecithin and Tween 20 for the encapsulation of bioactive carvacrol, Colloids Surf. A Physicochem. Eng. Asp. 517 (2017) 1–11, https://doi.org/10.1016/j.colsurfa.2016.12.056.
[21] S.Y. Choi, S.G. Oh, S.Y. Bae, S.K. Moon, Effect of short-chain alcohols as co-surfactants on pseudo-ternary phase diagrams containing lecithin, Korean J. Chem. Eng. 16 (3) (1999) 377–381, https://doi.org/10.1007/BF02707128.
[22] L. Deng, Current progress in the utilization of soy-based emulsifiers in, Foods 10 (6) (2021) 1354.
[23] M.J. Pascual-Villalobos, M. Cantó-Tejero, R. Vallejo, P. Guirao, S. Rodríguez-Rojo, M.J. Cocero, Use of nanoemulsions of plant essential oils as aphid repellents, Ind. Crops Prod. 110 (2017) 45–57, https://doi.org/10.1016/j.indcrop.2017.05.019.
[24] A. Marchese, R. Barbieri, E. Coppo, I.E. Orhan, M. Daglia, S.F. Nabavi, M. Izadi, M. Abdollahi, S.M. Nabavi, M. Ajami, Antimicrobial activity of eugenol and essential oils containing eugenol: A mechanistic viewpoint, Crit. Rev. Microbiol. 43 (6) (2017) 668–689, https://doi.org/10.1080/1040841X.2017.1295225.
[25] S.N. Ande, K.B. Sonone, R.L. Bakal, P.V. Ajmire, H.S. Sawarkar, Role of surfactant and co-surfactant in microemulsion: a review, Res. J. Pharm. Technol. 15 (10) (2022) 4829–4834, https://doi.org/10.52711/0974-360X.2022.00811.
[26] A. Fañani, B. Arcos-Álvarez, P. Banegas, L. Rocha, J. Monge-Corredor, R.G. Rubio, E. Guzmán, A. Lucia, Stabilization of gels and emulsions in the ternary water/eugenol/poloxamer 407-system: physicochemical characterization and potential application as encapsulation platforms, Colloids Surf. A Physicochem. Eng. Asp. 704 (4) (2025) 135474, https://doi.org/10.1016/j.colsurfa.2024.135474.
[27] I. Nikolic, E. Mitsou, I. Pantelic, D. Randjelovic, B. Markovic, V. Papadimitriou, A. Xenakis, D.J. Lunter, A. Zugic, S. Savic, Microstructure and biopharmaceutical performances of curcumin-loaded low-energy nanoemulsions containing eucalyptol and pinene: Terpenes' role overcome penetration enhancement effect? Eur. J. Pharm. Sci. 142 (ember 2019) (2020) 105135 https://doi.org/10.1016/j.ejps.2019.105135.
[28] S. Quintana-Martinez, A. Morales-Cano, L. García-Zapateiro, Rheological behaviour in the interaction of lecithin and guar gum for oil-in-water emulsions, Czech J. Food Sci. 36 (1) (2018) 73–80, https://doi.org/10.17221/315/2017-CJFS.
[29] P. Chivero, S. Gohtani, H. Yoshii, A. Nakamura, Effect of xanthan and guar gums on the formation and stability of soy soluble polysaccharide oil-in-water emulsions, Food Res. Int. 70 (2015) 7–14, https://doi.org/10.1016/j.foodres.2015.01.025.
[30] PREVAM PLUS (20 l.). - Fitoagricola. (n.d.). Retrieved November 24, 2025, from ⟨https://www.fitoagricola.es/prevam-20-l-461298⟩.
[31] M. Juttulapa, S. Piriyaprasarth, P. Sriamornsak, Effect of ph on stability of oil-in-water emulsions stabilized by pectin-zein complexes, Adv. Mater. Res. 747 (2013) 127–130, https://doi.org/10.4028/www.scientific.net/AMR.747.127.

[32] S. Rodríguez-Rojo, S. Varona, M. Núñez, M.J. Cocero, Characterization of rosemary essential oil for biodegradable emulsions, Ind. Crops Prod. 37 (1) (2012) 137–140, https://doi.org/10.1016/J.INDCROP.2011.11.026.
[33] Y. Cao, E. Dickinson, D.J. Wedlock, Creaming and flocculation in emulsions containing polysaccharide, Top. Catal. 4 (3) (1990) 185–195, https://doi.org/10.1016/S0268-005X(09)80151-3.
[34] X. Huang, Y. Kakuda, W. Cui, Hydrocolloids in emulsions: particle size distribution and interfacial activity, Food Hydrocoll. 15 (4–6) (2001) 533–542, https://doi.org/10.1016/S0268-005X(01)00091-1.
[35] E. Dickinson, C. Ritzoulis, Creaming and rheology of oil-in-water emulsions containing sodium dodecyl sulfate and sodium caseinate, J. Colloid Interface Sci. 224 (1) (2000) 148–154, https://doi.org/10.1006/jcis.1999.6682.
[36] G. Stojkov, Z. Niyazov, F. Picchioni, R.K. Bose, Relationship between structure and rheology of hydrogels for various applications, Gels 7 (4) (2021), https://doi.org/10.3390/gels7040255.
[37] K. Hyun, S.H. Kim, K.H. Ahn, S.J. Lee, Large amplitude oscillatory shear as a way to classify the complex fluids, J. NonNewton. Fluid Mech. 107 (1–3) (2002) 51–65, https://doi.org/10.1016/S0377-0257(02)00141-6.
[38] H. Yang, C.C. Tsai, J.S. Jiang, C.C. Hua, Rheological and textural properties of apple pectin-based composite formula with Xanthan gum modification for preparation of thickened matrices with dysphagia-friendly potential, Polymers 13 (6) (2021), https://doi.org/10.3390/polym13060873.
[39] Y.A. Shchipunov, E.V. Shumilina, Lecithin bridging by hydrogen bonds in the organogel, Mater. Sci. Eng. C. 3 (1) (1995) 43–50, https://doi.org/10.1016/0928-4931(95)00102-6.
[40] Q. Wang, P.R. Ellis, S.B. Ross-Murphy, The stability of guar gum in an aqueous system under acidic conditions, Food Hydrocoll. 14 (2) (2000) 129–134, https://doi.org/10.1016/S0268-005X(99)00058-2.
[41] K. Östbring, M. Matos, A. Marefati, C. Ahlström, G. Gutiérrez, The effect of ph and storage temperature on the stability of emulsions stabilized by rapeseed proteins, Foods 10 (7) (2021), https://doi.org/10.3390/foods10071657.